

Plasma Ignition and Combustion

Andreas Koleczko, Walter Ehrhardt, Stefan Kelzenberg, and Norbert Eisenreich*

Fraunhofer-Institut für Chemische Technologie (ICT), 76327 Pfinztal (Germany)

Summary

Electro-thermal-chemical (ETC) initiation and combustion offers the possibility to increase the performance of guns substantially as new propellant formulations and high loading densities (HLD) can be safely ignited and burnt in an augmented way. This paper reports investigations of burning phenomena in the low pressure region for JA2 and the effects of plasma interaction on ignition and study its influence on the burning rate. The comparison of transparent and opaque versions of the propellant is of special interest. Electrically produced plasma can strongly influence the ignition and combustion of solid propellants. Predominantly, plasma arcs influence strongly the burning of propellants by its radiation. The high intensity of the radiation initiates burning with short time delays in the μs -range and high conversion during exposure also in the case of a stable burning. Radiation can penetrate into the propellant interior and partially fragment at absorbing structures which could be artificially introduced or be inherently present as in the case of a JA2 propellant. Simplified approaches based on the heat flow equation and radiation absorption can explain these effects at least on a qualitative scale. Dynamic effects are understood by more sophisticated models.

1. Introduction

Electro-thermal-chemical (ETC) initiation and combustion^(1–8) offers to increase the performance of guns substantially as new propellant formulations and high loading densities (HLD) can be safely ignited and burnt in an augmented way. In basic research, the phenomena are studied in closed vessels which typically contain the solid propellant grains at loading densities up to 0.3 g/cm^3 . The propellant is ignited with plasma either introduced by a jet^(1–4) from a capillary or a cavity or by an arc from an exploding wire inside the propellant charge^(1,6–10). Measurements record current and voltage across the capillary, cavity or wire and pressure-time history in the chamber. The input of electrical power and energy into the vessel is directly derived from the measurements, but because of heat losses, it contributes to the enthalpy of the chamber gas. Therefore, the energy reaching the propellant by radiation or by hot reactive species is unknown. The propellant burning rates versus the pressure are calculated by analysing the pressure-time history using standard interior ballistic codes. These regression rates have indicated ETC augmentation of the burning

rate of solid propellants^(7,9–14). Solid propellant ETC guns achieved performance increases that could not only be explained by the added electrical energy⁽¹⁾. The augmentation can result from a modification in the inherent burn rate of the propellant caused by the plasma interaction, or by grain fragmentation resulting in an increase of the burning surface area. Recent results of experimental and theoretical investigations indicated that both concepts could be realized. The conventionally used burning rate descriptions like Vieille's law do not describe sufficiently the effects found in ETC ignition and combustion. Especially, radiation emitted from a plasma arc can strongly reduce ignition delay times and augment burning rates^(11–14).

It is the objective of this paper to report on investigations of burning phenomena in the low pressure region for JA2, the effects of plasma interaction on ignition and its influence on the burning rate. The comparison of transparent and opaque versions of the propellant is of special interest.

2. Simplified Theoretical Approach for Radiation Interaction

The explanation of important phenomena of plasma interaction on the ignition and combustion of solid propellants bases on the approach that the transition of the condensed phase to the gaseous phase dominates the ignition and burning of solid energetic materials. The non-affected solid heats up to the temperature of the burning surface caused by the energy transfer from the flame or other energy sources like radiation. The conversion to the gaseous phase can occur by endothermic evaporation, exothermic pyrolysis or heterogeneous reactions induced by some unspecified energy flux from the gaseous phase. The effects can be described by the heat flow equation whereas diffusion of species can be neglected.^(15–17) In the following, a radiative energy transfer Q_R is assumed in addition to the energy flux from the flame by conduction Q_0 .

In the case of an absorption of the total energy flux on the propellant surface which pyrolyses at a temperature T_p , an approximation for the ignition delay time t_{ign} can be found:

$$t_{ign} \approx \frac{\pi \lambda \rho c_p (T_p - T_0)^2}{4 \dot{Q}_R^2} \quad (1)$$

* Corresponding author; e-mail: Norbert.Eisenreich@ict.fhg.de

For a semi-transparent propellant with a unique absorption coefficient, a more complicated solution can be obtained. If the energy transfer is constant the following relation for the burning rate r can be derived:

$$r = \frac{\dot{Q}_0 + \dot{Q}_R}{\rho(c_p \cdot (T_s - T_0) + L - \sum_i q_i)} \quad (2)$$

Neglecting the phase transition and exothermic reactions in the condensed phase a formula for the burning rate can be given where the heat conduction from the flame \dot{Q}_0 is supposed to represent Vieille's law.

$$r = \frac{A \cdot p^n + \dot{Q}_R}{\rho(c_p \cdot (T_s - T_0))} \quad (3)$$

Eqs. (2) and (3) show that conductive and radiative heat transfer affect the burning rate in the same way. Eq. (3) enables to analyse the influence of physical and chemical parameters of solid propellants on ignition delay and linear burning rate. A least squares fit of burning rate data, measured at various initial temperatures T_0 , with Eq. (3) enables to obtain the unknown parameters T_s and \dot{Q}_0 ($\dot{Q}_R = 0$)⁽¹⁵⁾. It was found that Eq. (3) represents the temperature dependence of the linear burning rate of many solid propellants very well^(11,15). The fit parameter T_s lies systematically higher than the pyrolysis temperature obtained in thermal analytical experiments (e.g. TG or DSC). For JA2 T_s was found to be rather constant and close to 675 K⁽¹⁵⁾, and the conductive heat flux from the flame to the propellant surface increased from 6000 W/cm² to 15 000 W/cm² at pressures from 70 to 175 MPa.

Ignition, burning rates and their pressure dependence were calculated also by the method of Zarko and Rychkov^(19,20). They developed a one-dimensional computer code CTEM (Combustion Transients of Energetic Materials) which takes into account time-dependent phenomena of condensed propellants subjected to the time-variable heat flux. CTEM can include a solid and a liquid phase allowing the solid propellant to melt and evaporate at the surface. Depending on the optical properties of the propellant the radiant flux is absorbed at the surface or in the depth of the condensed material. Chemical conversions can occur both in the condensed and gas phases. In the gaseous phase, in addition to the heat flow, the diffusion of three species is allowed. CTEM was successfully applied to the ignition and combustion of nitromethane and the response of a nitramine propellant to energy pulses from external sources^(16,18,21). Figures 1 and 2 show the response on a heat flux absorbed at the surface (Figure 1) and in the interior of the propellant (Figure 2).

The mass conversion of porous and foamed propellants deviates also from Vieille's law. The conversion rates are essentially above those obtained by the linear burning of the compact energetic materials. Some theoretical approaches assume hot gases of the flame to penetrate the porous solid according to Darcy's law, Eq. (4), their velocity is proportional to the pressure gradient and the permeability of the material (inverse if drag resistance k_d is used).

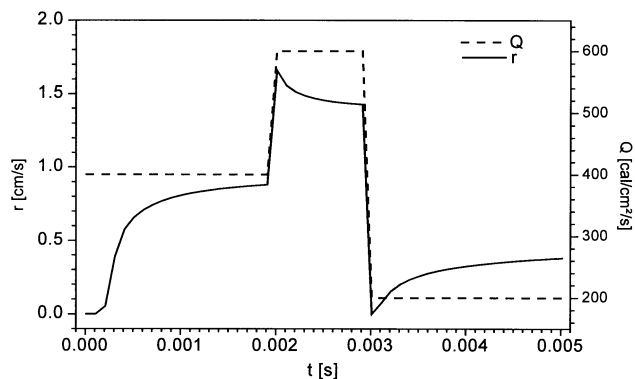


Figure 1. Transient burning rate of a solid propellant (physical data of RDX) on an external heat flux absorbed at the surface.

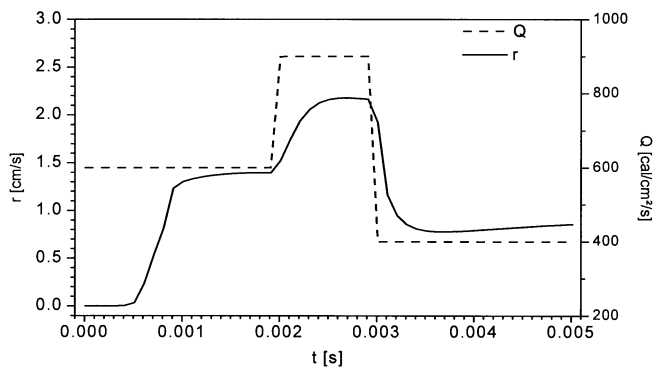


Figure 2. Transient burning rate of a solid propellant (physical data of RDX) on an external heat flux absorbed in the depth of the propellant.

$$\nabla p = -k_d v_{hg} \quad (4)$$

The gases generate hot spots in the propellant pores which evolve to (quasi) spherical burning zones consuming the propellant at larger burning surfaces. Taking into account stand-off distances of the flame which depend on pressure (Refs. 18, 22, 23) the porous burning occurs only if these distances are lower than the pore sizes⁽²⁴⁾.

$$\frac{dp}{dt} \propto \frac{dm}{dt} = 4\pi\rho \sum_{i,j,k} r_{i,j,k}^2(t) \frac{dr_{i,j,k}}{dt} \quad (5)$$

$r_{i,j,k}$ within penetration depth

Using a highly simplified approach of the heat flow equation a three-dimensional calculation can give the conversion of the solid based on overall chemical kinetics and heat of reaction^(25–28). The hot spots are approximated by a sum of Gaussian curves which would result from a δ -function energy input at $\vec{x}_{i,j,k}$ developing in time (see e.g. solution by integration with Green's function in Refs. 25–28):

$$T_{hs}(\vec{x}, t) = \sum_{i,j,k=1}^{I,J,K} \frac{Q_{i,j,k} e^{-[(\vec{x}-\vec{x}_{i,j,k})^2/4(t-t_{i,j,k})]}}{(4\pi(t-t_{i,j,k}))^{3/2}} \quad t_{i,j,k} > t'' \quad (6)$$

A propagating hot gas flow with speed v_{hg} initiates hot spots at time $t_{n,j,k}$ possibly including a response time t_R ($=0$, here):

$$t_{n,j,k} = t_{n-1,j,k} + \frac{x_{n,j,k} - x_{n-1,j,k}}{v_{hg}} + t_R \quad (7)$$

Chemical reactions of the Arrhenius type lead to a non-linear behaviour of the heat flow equation which can no longer be solved analytically. An initial temperature distribution is converted to an instantaneous heat source that would provide this temperature distribution. Chemical reactions take place which, in addition, contribute to the instantaneous heat sources.

Hot spots which form pores or lead to in-depth ignition could be obtained by a radiative energy source of the following type (linear to form layers at regular distances in this case):

$$\dot{Q}[x, t] = \sum_{i=1}^I \dot{Q}_R \cdot b \cdot e^{-b \cdot i \cdot d} \cdot \sqrt{\frac{\rho \cdot c_p}{2\pi\lambda t}} \cdot e^{-[\rho \cdot c_p \cdot (x-i \cdot x_d)^2 / 2\lambda t]} \quad (8)$$

The temperature development in the energetic solid material is calculated as described in Refs. 25–28.

3. Experiments

For the experiments two types of JA2 were used:

- (1) The standard formulation containing carbon and
- (2) A transparent version with the same composition but without carbon.

The shapes of the propellants were plates of 3 mm thickness and 20 mm breadth. These plates were formed to rings put into a plastic tube (polyamide). The plastic tube fitted into the closed vessel and the outer surface was at a distance of 20 mm to the exploding wire. The distance of the wire to the inner surface of the propellant was 17 mm.

The propellants were investigated in two types of chambers:

- (1) A closed vessel was used with a volume of 100 ml (most experiments at a loading density of 0.117 g/cm^3 , $T_0 = 293 \text{ K}$), enabling the registration of the pressure-time behaviour at different loading densities. The plasma initiation was performed by a wire explosion in the axis of the bomb. The wire was contacted by electrodes at a distance of 40 mm (Figure 3).
- (2) An ‘‘optical’’ bomb is equipped with windows and can withstand pressures up to 13 MPa. It was used for photographic studies of the burning zones and spectroscopic investigations. The experimental setup is described in detail in other publications^(29,30).

A 100 kJ power supply with maximum voltages of 22 kV enabled ETC ignition and combustion whereas only stored energies up to 10 kJ were used. The resistor was $< 10 \text{ m}\Omega$ and the inductivity was $20 \text{ }\mu\text{H}$. The plasma was produced by a wire explosion igniting or pre-treating the propellant. Successive pulses could occur which influence the stabilized burning mode. The voltage was measured at the electrodes and the current by a Rogowsky Coil. The signal data were acquired by a 4 channel transient recorder with sampling rates up to 100 MHz.

The burning rates were calculated from the pressure-time curves according to the procedures described in Refs. 31–32.

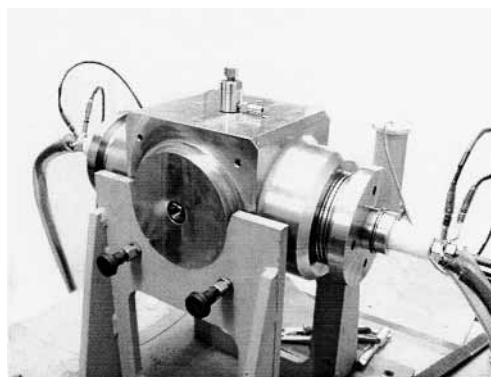


Figure 3. Closed vessel for the plasma interaction studies.

In the case of the simple geometry of the plates the burning rates or apparent burning rates were estimated from the pressure maximum which was related to the thickness of the JA2 and the first derivative of the pressure-time curve ignoring the influence of the boundaries of the propellant stripe, the true equation of state of the gases and the cooling by energy loss to the bomb volume.

In addition, the JA2 plates were pre-treated applying ‘‘open’’ conditions which means that the same plastic tubes were prepared with the propellant stripes outside the closed vessel and then the plasma arc initiated by the wire explosion.

The vessel was equipped with one fiber optical system pressure transducer. For interrupted burning tests, a special closed chamber was used with a plug containing a stainless steel rupture disc. In this chamber propellants were investigated which were pre-treated in the ‘‘open’’ experiments.

4. Comparison of the Ignition of Transparent and Black JA2

In preliminary experiments it was found that the burning rates of black and transparent JA2 are equal if they are not ignited by plasma or pre-treated by plasma in an open experiment.

Figure 4 shows the pressure-time curves of experiments where black and transparent JA2 were subjected to a plasma arc of 2 kJ and where transparent JA2 was initiated by 1 g

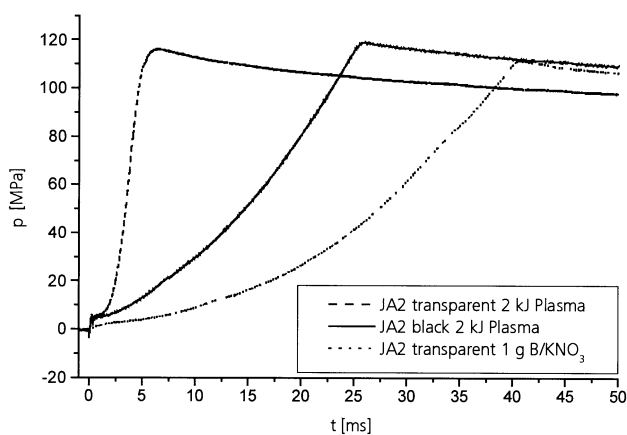


Figure 4. Comparison of plasma and pyrotechnic ignition of black and transparent JA2.

B/ KNO_3 . The ignition delay indicated by an initial pressure rise is similar for both cases of plasma ignition and essentially faster than that of the conventional ignition. The pressure increase is similar for the black JA2 ignited by plasma and the JA2 ignited by B/ KNO_3 resulting in similar burning rates. The conversion of the solid material is accordingly higher on the plasma pulse. The ignition delay decreases with increasing electrical energy fed to the arc. The pressure increase which is roughly proportional to the apparent burning rate in the setup used is strongly enhanced for transparent JA2.

Results of discharged energies of 1 kJ, 2 kJ and 6 kJ applied to transparent JA2 are plotted in Figure 5. Using

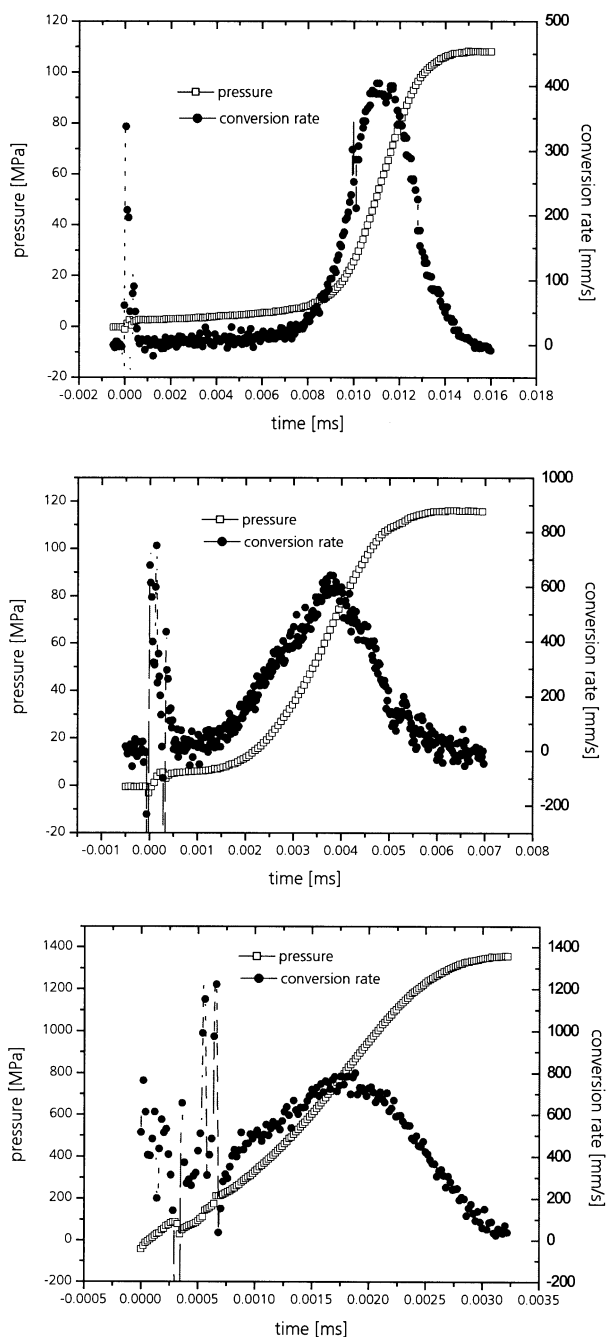


Figure 5. Comparison of the pressure-time curves and conversion rates of the ignition of transparent JA2 with various electric energies 1 kJ (top), 2 kJ (middle), 6 kJ (bottom).

the lowest energy of 1 kJ, a long time period occurs where JA2 burns with the normal low pressure burning rate after the end of the electrical pulse (see also Figure 9). When reaching a pressure of 6 to 8 MPa a strong increase of the apparent burning rate is found. The pressure of 6 to 8 MPa is reached fast with an electrical energy of 2 kJ and the period of normal burning is short. After a discharge of 6 kJ only a strongly enhanced burning is observed.

The following hypothesis on plasma ignition of JA2 is proposed:

- Black JA2: a short ignition time is obtained, only at high radiant fluxes in depth effects could be observed
- Transparent JA2: a short ignition time is obtained, plasma radiation forms a porous structure in the interior of the propellant causing a successive porous combustion characteristics
- Ignition delay times and burning rate enhancement follow at least qualitatively the theoretical approaches described above.

5. Transmission of JA2

The transmission of radiation through transparent JA2 plates has been investigated and the results are plotted for various conditions in Figure 6. Transparency begins close to 400 nm and increases with increasing wavelength. A surface treatment reducing the roughness increases the transmission substantially. The radiation effects in the interior of the propellant are obviously induced by the radiation of the visual, NIR or IR spectral range. An open experiment verified this findings by partially covering the JA2 sample with a PMMA plate which shows a steep absorption edge close to 400 nm. Indeed, the PMMA plate did not change the effects observed in the interior.

6. Pre-Treatment of Transparent JA2

JA2 was pre-treated by plasma discharge after wire explosion in open experiments where 0.8 or 1.5 kJ energy

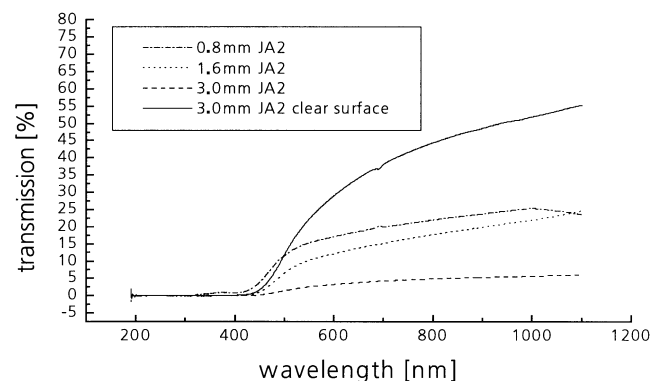


Figure 6. Transmission spectra of transparent JA2.

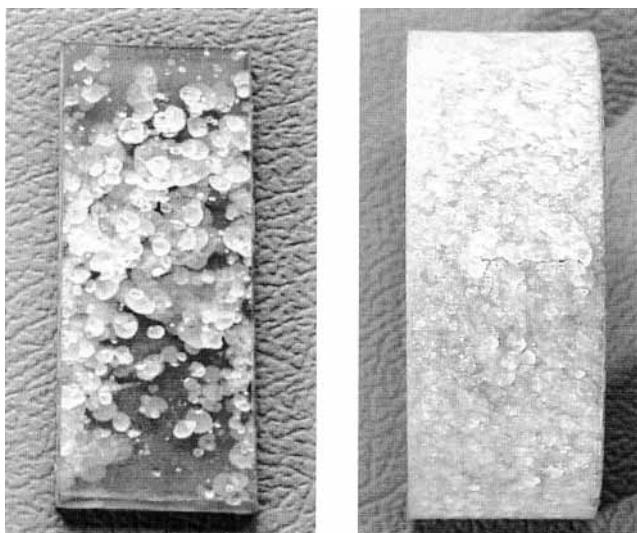


Figure 7. Pre-treated transparent JA2 by a plasma arc (left: wire explosion in the middle above a flat sample; right: wire explosion centered in a tubular sample).

were applied. Black JA2 ignited and burned under these conditions.

The transparent pre-treated JA2 plates show effects of fragmentation in the interior which are lens shaped crazes of a diameter of 2 mm or less. They are orientated parallel to the rolling direction during the production of the JA2 plates (possible due to the orientation of the nitrocellulose fibres). Pictures of the pre-treated material are shown in Figure 7. The following experiments were performed with the pre-treated JA2 plates:

1. Observation of the burning behaviour by a video camera and measurement of the burning rate in the optical bomb: The video frames which are shown in Figure 8 indicate that the flame front is not linear but penetrates into the crazes forming a broad flame zone still in the solid at higher pressures. The depth increases when the pressure increases. The apparent burning rate is higher than that of non-treated JA2 at 4 and 7 MPa. The apparent

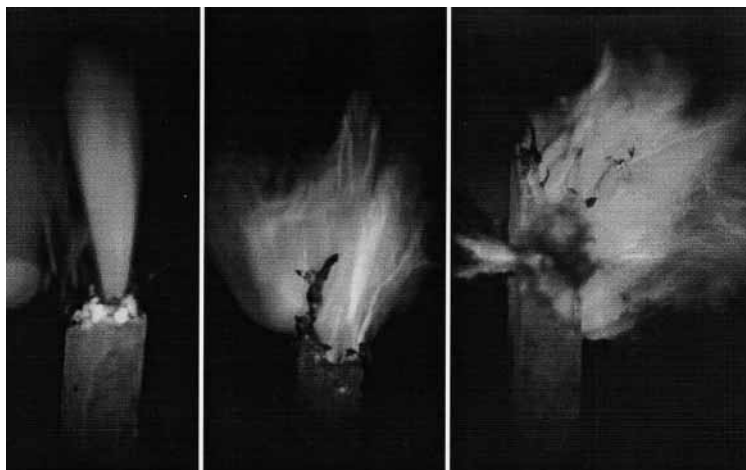


Figure 8. Pre-treated transparent JA2 (1.8 kJ) studies in an optical bomb at pressures of 20, 40 and 100 MPa (from left to right). Burning occurs in the volume of the not yet fully pyrolysed propellant.

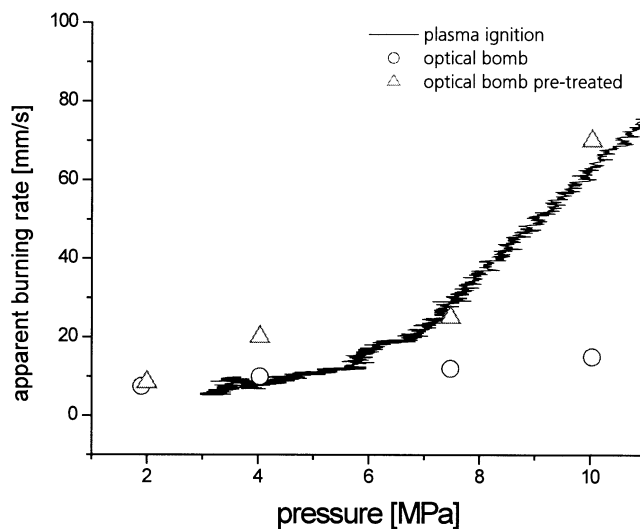


Figure 9. Apparent burning rate of transparent JA2 ignited by a 1 kJ electrical pulse: obtained from ignition in the plasma vessel compared to the burning rate of transparent JA2, pre-treated by a 1 kJ plasma and without plasma pre-treatment measured in an optical bomb.

burning rate obtained from the experiment in the plasma bomb shown in Figure 5 using 1 kJ electrical energy agrees well with the (apparent) burning rate measured in the optical bomb (see Figure 9).

2. A detailed analysis of the pressure-time curves obtained by 1 and 2 kJ plasma arc ignition in the closed vessel results in a similar behaviour of the burning rate depending on pressure. There is an increase of the apparent burning rate (or conversion rate) after 4 MPa and dramatically after 7 MPa above that of black JA2.
3. If ignited by 1 g B/KNO₃ the pre-treated transparent JA2 exhibits the same burning behaviour as if ignited untreated by a plasma arc.
4. Experiments with burning interruption were performed. They indicate that the burning takes place in the lens shaped crazes and voids whereas the solid keeps its outer shape (see Figure 10).

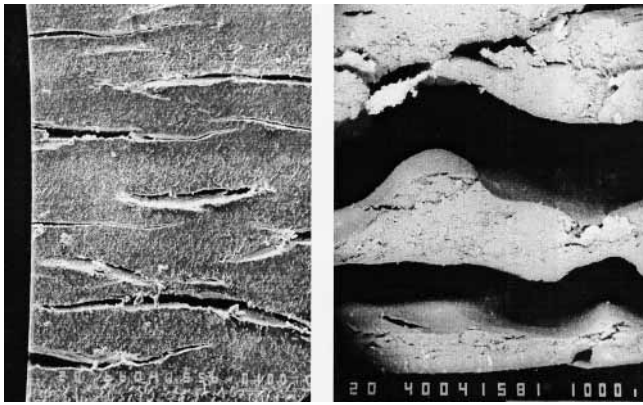


Figure 10. REM pictures of the crazes generated by the plasma radiation in transparent JA2 before burning (left), and after burning interruption (right) for conventional ignition.

7. Response of Black JA2 on Plasma Pulses

The effect of plasma pulses was investigated by exposing the propellant to one or more arc discharges firstly initiated by the wire explosion. A step by step pressure increase occurs directly related to the electrical pulses and could be caused by the increase of temperature and/or by ablation of plastic material from the tube. There is only a very short time delay between the electrical pulses and the pressure increase of about 100 or 200 μs . Assuming a reasonable energy transfer (about 10%) by plasma radiation to the atmosphere and the plastic material, delay times of less than 100 μs are expected by Eq. (1) which is in accordance with the experimental results. The regression rate Eqs. (2) and (3) of the solid can occur independently of a chemical reaction of the material.

In the case of black JA2 which absorbs radiation predominantly on the surface, a result is shown in Figure 11. There are small time shifts between pressure increase and the electrical pulses at an order of magnitude of 100 μs . Conversion rates on the electrical pulses are between 500 to 2000 mm/s. Assuming a conversion of the propellant material according to Eqs. (2) or (3) the energy reaching the propellant surface is estimated to be between 75 and

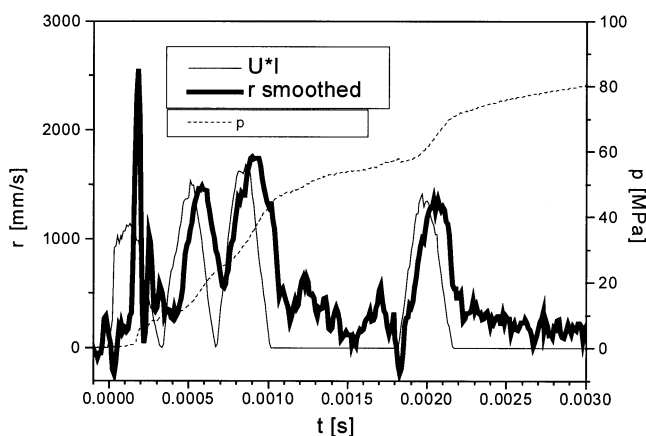


Figure 11. Electrical power, pressure-time curve and conversion rates of black JA2.

350 kW/cm² which corresponds to an efficiency of the transfer of electrical energy of 10 to 20%. A detailed analysis will be done according to a sophisticated procedure to describe plasma radiation effects^(33–35). The subsequent burning after the electrical pulses takes place according to the “normal” burning of JA2 with the “normal” burning rates. The pressure exponent found in these cases was between 0.65 and 0.74 (see Figure 12) below 75 MPa. The lower pressure exponents were found for the treatment with higher electrical energy. In cases of higher electrical pulses (> 2 kJ, see Figure 12) the transition to the “normal” burning was delayed and occurred at higher apparent burning rates which additionally fluctuate when the described experimental conditions are applied. The absorption coefficient of black JA2 does not vanish completely, and, evidently, very strong radiation still penetrates the interior of the propellant. Although strongly weakened, it could cause some crazes and fragmentation as in the case of transparent JA2 and influence the conversion.

8. Modelling the Porous Burning of Transparent JA2

The burning rate dependence of transparent JA2 with plasma treatment is qualitatively described by the following model:

1. The plasma pulse (as pre-treatment or in the ignition phase) causes crazes and voids in the interior of the propellant which later act as hot spot centres of burning.
2. If the initial pulse does not cause a pressure increase above 2 to 3 MPa then a “normal” linear burning begins including hot spots at the surface. The burning rate does not exceed the burning rate of normal JA2.
3. The pressure gradient between the propellant interior and the closed volume drives hot reaction products into the porous structure (see Eq. (4)) which cause conversion (Eq. (5)) and burning in the case that the flame quenching distance or the flame stand-off distance is below the size of the pores (crazes, voids).

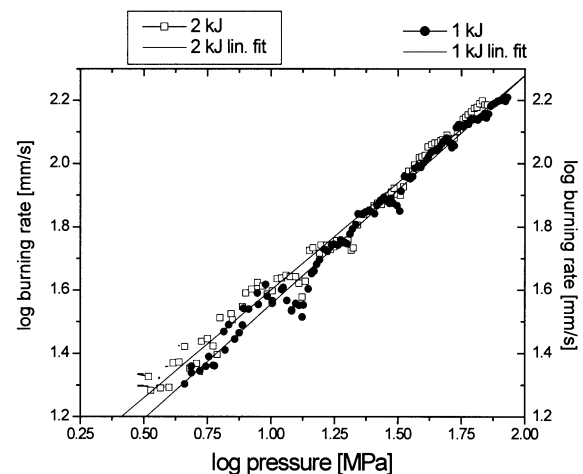


Figure 12. Burning rates of JA2 at pressures below 75 MPa, pressure exponents are 0.72 after the plasma ignition of black JA2 by an electrical pulse with 1 kJ ● and 0.67 after a pulse of 2 kJ □.

4. This case is realized above 4 to 7 MPa and the burning occurs within a volume between the surface and a depth where the hot gases can penetrate into pores. At pressures of 4 to 7 MPa the flame stand-off distance decreased already below 1 mm.

The hot spot mechanism reported above can describe this behaviour on a qualitative scale, physical and chemical of JA2 and the kinetics of nitrocellulose decomposition were used^(24–26). The experimental data of Figure 5 indicate that the enhanced burning occurs immediately in the case of 6 kJ electrical energy applied and shortly after the end of the pulse on 2 kJ. On 1 kJ a long normal burning is found till a pressure of 4 to 7 MPa is reached.

The ignition is initiated by hot spots (Eq. (6)) which could be pores on the surface. At the beginning shortly a stable burning with a constant burning rate is obtained. After an amount of material conversion to be chosen a hot spot array (Eq. (6)) is set in front of the burning surface in the non-reacted propellant where the individual hot spots spherically enlarge by conversion (Eq. (5)). At increasing total conversion (pressure) the rate of setting further hot spot arrays increases (see Eqs. (4) and (7)). The consequence is that at higher total conversion (pressure) a broader volume of the propellant contributes to the burning progress and the pressure increase (Eq. (5)).

The results of numerical calculations studying a linear progression of the porous burning in a solid energetic material with a grid of $50 \times 50 \times 500$ points are shown in Figures 13 and 14. In Figure 13 the pressure initially increases slowly according to the normal linear burning rate. After a certain conversion (in this case a fraction of 0.2 of the total volume) hot spots are set in the interior of the solid propellant ahead of the burning surface. The conversion of the propellant then increases strongly with time. In Figure 14 hot spots are initiated directly after the ignition and form peaks in the curve of the apparent burning rate curve (conversion rate). These peaks emerge

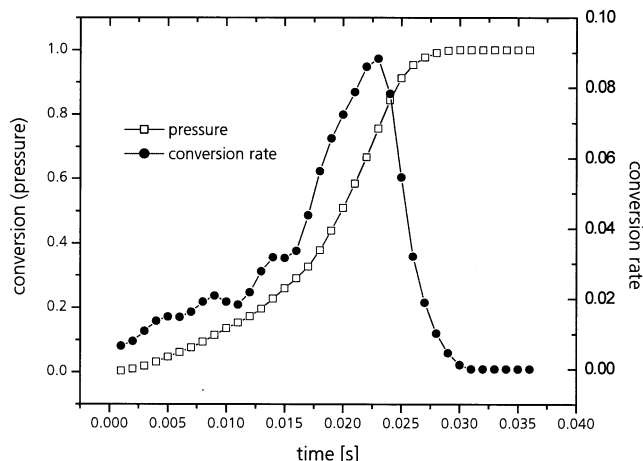


Figure 14. Conversion which corresponds to a normalized pressure calculated by the hot spot model of porous propellants: penetration of hot gases into the solid material without a delay.

to a strong peak at high (up to 2 orders of magnitude) total conversion (pressure) when the hot spots are set faster. This indicates the simultaneous burning of hot spot arrays at different individual conversion. The results are similar, at a qualitative level, to the experimental findings of apparent burning rates depending on time and pressure. The temperature distribution in the x - z plane is illustrated in Figure 15 where the reaction propagates with hot spots at different stages of the reaction. The hot spots at the leading edge of the reaction zone develop to larger holes where the combustion has completed. Later they emerge to form a continuous gaseous phase zone.

9. Fragmentation at Elements of Absorbing Structures

Transparent JA2 can be directly pre-treated during the plasma ignition. Its burning characteristics are modified

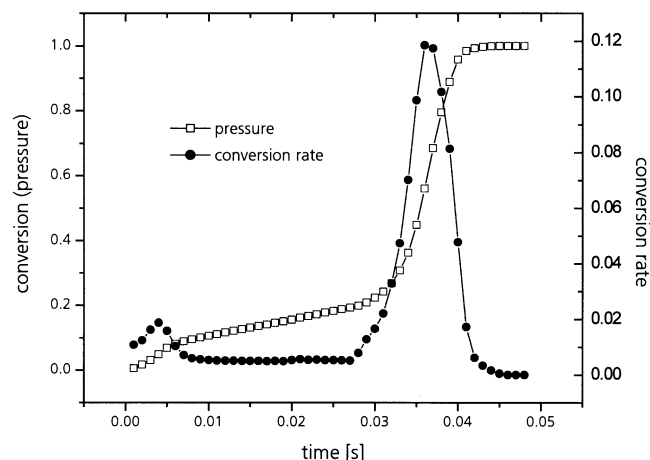


Figure 13. Conversion which corresponds to a normalized pressure calculated by the hot spot model of porous propellants: up to 0.03 s (0.2 conversion) a normal linear burning occurs, at a conversion of 0.2 hot gases penetrate into the solid material to fill the crazes and void in the interior and therefore form hot spots.

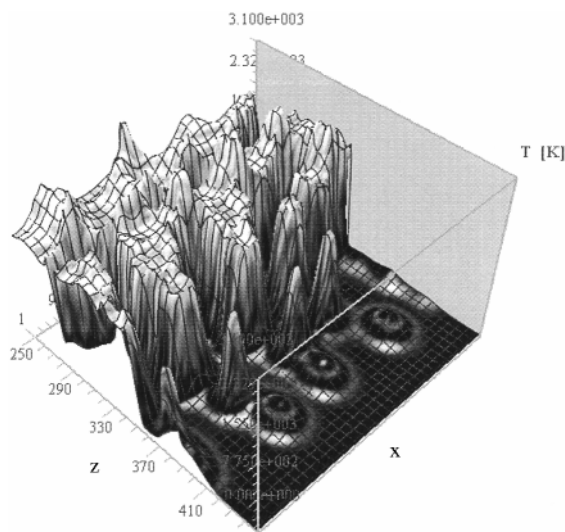


Figure 15. Temperature distribution in x - z -plane of an energetic material where the reaction propagates with hot spots successively initiated (in a stage where porous burning is already developed).



Figure 16. Plasma fragmentation of two JA2 stripes in an “open” experiment.

depending on the intensity of the plasma pulse. In generally, in transparent propellants photo absorbing centres or structures could serve to form hot spots on high intensity radiation. Simply carbon particles, fibres or layers are appropriate, as well as, more sophisticated, photo active substances. Theoretically, the hot spot models can qualitatively describe the effects. The absorption by the centres or structures and the absorption of the propellant layers between them and the surface can be described by a hot spot approach (see Eq. (8)). The subsequent development of the hot spots and the conversion occurs according to Eq. (7). The effect was already realized in an open experiment. Two stripes of transparent JA2 were connected by a carbonized layer using a solvent. As expected a plasma pulse of 2 kJ split the stripes at the black layer (see Figure 16).

10. Conclusion

Plasma can influence the ignition and combustion of solid propellants. Especially, plasma arcs interact strongly by their radiation with propellants. The high intensity of the radiation initiates burning with short time delays in the μs -range and high conversion during exposure also in the case of a stable burning. If the radiation can penetrate into the propellant interior partial fragmentation by absorbing structures occurs which could be artificially introduced or be inherently present as in the case of a double base propellant.

Simplified approaches based on the heat flow equation and radiation absorption can explain these effects at least on a qualitative level. Dynamic effects are understood by more sophisticated models.

11. References

- (1) Th. H. G. G. Weise, “German Nation Overview”, *10th Electromagnetic Launch Symposium*, San Francisco, California, 25–28 April, 2000.
- (2) C. R. Woodley and S. Fuller, “Apparent Enhanced Burn Rates of Solid Propellants Due to Plasmas”, *16th International Symposium on Ballistics*, San Francisco, CA, USA, September 23–28, 1996, pp. 153–162.
- (3) W. G. Proud and N. K. Bourne, “The Electrothermal Enhancement of Propellant Burning by Plasma Injection”, *Propellants, Explosives, Pyrotechnics*, 22, 212–217 (1997).
- (4) A. Bach, N. Eisenreich, and M. Neiger, “Charakterisierung eines Plasma-Jets mit optischen und spektroskopischen Methoden”, *22nd Int. Ann. Conf. of ICT*, Karlsruhe, Germany, July 2–5, 1991, pp. 98.1–10.
- (5) M. J. Taylor, “Measurement of the Properties of Plasma from ETC Capillary Plasma Generators”, *10th Electromagnetic Propellants, Explosives, Pyrotechnics* 26, 75–83 (2001)
- (6) P. J. Kaste *et al.*, “ETC Plasma-Propellant Interactions”, *29th Int. Annual Conference of ICT*, Karlsruhe, Germany, June 30–July 3, 1998, pp. 125.1–14.
- (7) H. K. Haak, A. M. Voronov, and Th. H. G. G. Weise, “The Interaction of Electrothermally Supplied Energy with Compact Solid Propellants”, *9th EML Symposium*, Edinburgh, Scotland, UK, May 13–15, 1998.
- (8) W. F. Oberle and G. P. Wren, “Radiative and Convective Heat Loss in Electrothermal-Chemical (ETC) Closed Chambers”, *35th JANNAF Combustion Subcommittee Meeting*, Tucson, AZ, USA, December 1998, Vol. I, pp. 229–236.
- (9) D. E. Kooker, “Burning Rate Deduced from ETC Closed-Chamber Experiments: Implications for Temperature Sensitivity of Gun Systems”, *35th JANNAF Combustion Subcommittee Meeting*, Tucson, AZ, December 1998, Vol. II, pp. 201–217.
- (10) A. Birk, M. Del Guercio, A. Kinkennon, D. E. Kooker, and P. J. Kaste, “Interrupted-Burning Tests of Plasma-Ignited JA2 and M30 Grains in a Closed Chamber”, *Propellants, Explosives, Pyrotechnics*, 25, 133–142 (2000).
- (11) A. Koleczko, W. Eckl, and T. Rohe, “Untersuchungen zur Einkopplung elektrischer Energie in flüssige Energieträger und deren Verbrennungsprodukte”, *27th International Annual Conference of ICT*, Karlsruhe, Germany, June 25–28, 1996, pp. 142.1–21.
- (12) A. Voronov, A. Koleczko, H. Haak, Th. Weise, and N. Eisenreich, “Energy Criteria for Combustion control in a large caliber gun”, *IEEE Trans. on Magn.* (in press).
- (13) A. Voronov, *et al.* “The Interaction of Electrothermally Supplied Energy with Compact Solid Propellants”, *IEEE Trans. on Magn.*, 35, No.1, 224–227, (1999).
- (14) N. Eisenreich, W. Ehrhard, S. Kelzenberg, A. Koleczko, and H. Schmid, “Strahlungsbeeinflussung der Anzündung und Verbrennung von festen Treibstoffen”, *31st Int. Annual Conference of ICT*, Karlsruhe, Germany, June 27–30, 2000, pp. 139.1–19.
- (15) N. Eisenreich, *Vergleich theoretischer und experimenteller Untersuchungen über die Anfangstemperaturabhängigkeit von Festtreibstoffen*, ICT-Bericht 8/77, Fraunhofer-Institut für Chemische Technologie (ICT), Pfanztal, Germany, (1977).
- (16) W. Eckl, S. Kelzenberg, V. Weiser, and N. Eisenreich, “Einfache Modelle der Anzündung von Festtreibstoffen”, *29th Int. Annual Conference of ICT*, Karlsruhe, Germany, June 30–July 3, 1998, pp. 154.1–20.
- (17) N. Eisenreich, T. S. Fischer, and G. Langer, “Burning Rate Models of Gun Propellants”, *European Forum on Ballistics of Projectiles*, Saint Louis, France, April 11–14, 2000, pp. 117–127.
- (18) N. Eisenreich, W. Eckl, Th. Fischer, V. Weiser, S. Kelzenberg, G. Langer, and A. Baier, “Burning Phenomena of the Gun Propellant JA2”, *Propellants, Explosives, Pyrotechnics*, 25, 143–148 (2000).
- (19) V. E. Zarko, L. K. Gusachenko, and A. D. Rychkov, “Simulation of Combustion of Melting Energetic Materials”, *Defence Science Journal*, 46, No. 5, 425–433 (1996).
- (20) L. K. Gusachenko, V. E. Zarko, and A. D. Rychkov, “Modeling of Gasification of Evaporated Energetic Materials under Irradiation”, *INTAS Workshop*, Milan, Italy, July 1996.
- (21) S. Kelzenberg, N. Eisenreich, W. Eckl, and V. Weiser, “Modelling Nitromethane Combustion”, *Propellants, Explosives, Pyrotechnics*, 24, 189–194 (1999).
- (22) N. Kubota, T. J. Ohlemiller, L. H. Caveny, and M. Summerfield, “The Mechanism of Super-Rate Burning of Catalyzed Double Base Propellants”, *15th Symposium (International) on Combustion*, Tokyo 1974, pp. 529–537.
- (23) N. Eisenreich, “A Photographic Study of the Combustion Zones of Burning Double Base Propellant Strands”, *Propellants and Explosives*, 5, 141–146 (1978).
- (24) T. S. Fischer, W. Koppenhöfer, G. Langer, and M. Weindel, “Modellierung von Abbrandphänomenen bei porösen Ladungen”, *30th International Annual Conference of ICT*, Karlsruhe, Germany, June 29–July 2, 1999, pp. 98.1–13.

- (25) N. Eisenreich and A. Pfeil, "Pyrolysis Craters Produced by Laser Pulse Irradiation on Propellant Solids", *Appl. Phys.*, 15, 47 (1978).
- (26) N. Eisenreich, "Successively Initiated Arrays of Hot Spot in a Reactive Medium", *Proc. Physics of Explosives*, Berchtesgaden, September 29–October 1, 1997.
- (27) G. Langer and N. Eisenreich, "Entwicklung von Hotspots in energetischen Materialien", *29th International Annual Conference of ICT*, Karlsruhe, Germany, June 30–July 3, 1998, pp. 157.1–9.
- (28) G. Langer and N. Eisenreich, "Hot Spots in Energetic Materials", *Propellants, Explosives, Pyrotechnics*, 24, 113–118 (1999).
- (29) N. Eisenreich, H. P. Kugler, and F. Sinn, "An Optical System for Measuring the Burning Rate of Propellant Strands", *Propellants, Explosives, Pyrotechnics*, 12, 78–80 (1987).
- (30) W. Eckl, V. Weiser, G. Langer, and N. Eisenreich, "Burning Behaviour of Nitramine Model Formulations", *Propellants, Explosives, Pyrotechnics*, 22, 148–151 (1997).
- (31) H. Krier and S. A. Shimpi, "Predicting Uniform Gun Interior Ballistics Part I: An Analysis of Closed Bomb Testing", Technical Report AAE 74-5, (1974), Aeronautical and Astronautical Engineering Department University of Illinois at Urbana-Champaign, USA (1974).
- (32) M. Hund, N. Eisenreich, and F. Volk, "Determination of Interior Ballistic Parameters of Solid Propellants by Different Methods", *Proc. 6th Int. Symp. on Ballistics*, Orlando, USA, 1981, pp. 77–84.
- (33) K. Kappen and U. H. Bauder, "Simulation of Plasma Radiation in Electrothermal-Chemical Accelerators", *IEEE Transactions on Magnetics*, 35, 1, 192–196 (1999).
- (34) K. Gruber, K. Kappen, A. Voronov, and H. Haak, "Radiation Absorption of Propellant Gas", *10th Electromagnetic Launch Symposium*, San Francisco, California, April 25–28, 2000.
- (35) K. Kappen and U. H. Bauder, "Calculation of Plasma Radiation Transport for Description of Propellant Ignition and Simulation of Interior Ballistics in ETC Guns", *10th Electromagnetic Launch Symposium*, San Francisco, California, April 25–28, 2000.

Symbols

t_{ign}	ignition delay time
λ	heat conductivity
ρ	density
c_p	heat capacity
T_p	pyrolysis temperature
T_0	initial temperature
r	burning rate
Q_r	radiative energy flux
Q_0	conductive energy flux
L	latent heat of evaporation
q	reaction energy
T_s	surface temperature
p	pressure
A	pre-exponential factor
n	pressure exponent
k_d	drag resistance
v_{hg}	velocity of hot gases
t	time
m	mass
$r_{i, j, k}$	radius of hotspot i, j, k
T_{hs}	temperature distribution of hot spots
x	space coordinate
t_R	response time

(Received January 23, 2001; Ms 2001/005)